Galama, T.J., Vreeswijk, P., van Paradijs, J., et al., 1998, Nature 395, 670.
Galama, T.J., Vreeswijk, P.M., Rol, E. et al., 1999, GCN #388.
Galama, T.J., Tanvir, N., Vreeswijk, P., et al., 2000, *ApJ.* in press.
Hjorth et al. 2000, in press.
in 't Zand, J., Heise, J., Hoyng, P., et al., 1997, *IAU Circular* #6569.
Jensen, B. L., et al., 2000, in preparation.
Kulkarni, S., Djorgovski, S. G., Ramaprakash, A. N., et al., 1998, *Nature* **393**, 35.
Leibundgut, B., Sollerman, J., Kozma, C., et al., 2000, *The Messenger*, **99**, 36.
Masetti, N., Palazzi, E., Pian, E., et al., 2000, *A&A* **354**, 473.
Mészáros, P., and Rees, M.J., 1997, *ApJ.* **476**, 232.
Palazzi, E., Pian, E., Masetti, N., et al., 1999, *A&A* **336**, L95.
Pedersen, H., Jensen, B.L., Hjorth, J., et al., 2000, *GCN* #534.
van Paradijs, J., Groot, P.J., Galama, T.J., et al., 1997, *Nature* **386**, 686.
Vreeswijk, P.M., Rol, E., Hjorth, J., et al., 1999a, *GCN* #496.
Vreeswijk, P.M., et al., 1999b, *ApJ* submitted.
Wijers, R.A.M.J., Rees, M.J., and Mészáros, P., 1997, *M.N.R.A.S.*, **288**,L51.
Wijers, R.A.M.J., Vreeswijk, P.M., Galama, T.J., et al., 1999, *ApJ.L*. 523, L33.

ISAAC on the VLT Investigates the Nature of the High-Redshift Sources of the Cosmic Infrared Background

Two jewels of European astronomy, ISO and ISAAC, join their capabilities to shed light on one important enigma of present-day cosmology

D. RIGOPOULOU[1], A. FRANCESCHINI[2], H. AUSSEL[3], C.J. CESARSKY[4], D. ELBAZ[5], R. GENZEL[1], P. VAN DER WERF[6], M. DENNEFELD[7]

[1]Max-Planck-Institut für Extraterrestrische Physik, Garching, Germany
[2]Dipartimento di Astronomia, Università di Padova, Vicolo Osservatorio, Padova, Italy
[3]Osservatorio Astronomico di Padova, Vicolo Osservatorio, Padova, Italy
[4]European Southern Observatory, Garching, Germany
[5]CEA Saclay, Gif-sur-Yvette Cédex, France
[6] Leiden Observatory, Leiden, The Netherlands
[7]Institut d'Astrophysique de Paris – CNRS, Paris, France

Abstract

We report on the status of our long-term project aimed at characterising the nature of a new population of galaxies that has emerged from various ISOCAM surveys[1]. In September 1999, we used ISAAC on UT1 and under very good seeing conditions over two nights we obtained the first near-infrared spectra for a sample of ISOCAM galaxies drawn from a deep ISO survey of the Hubble Deep Field South. The Hα emission line was detected in 11 out of the 12 galaxies we looked at, down to a flux limit of 7×10^{-17} erg cm^{-2} s^{-1}, corresponding to a line luminosity of 10^{41} erg s^{-1} at $z = 0.6$ (for an $H_0 = 50$ and $\Omega = 0.3$ cosmology). The rest frame R-band spectra of the ISOCAM galaxies we observed resemble those of powerful dust-enshrouded starbursts. The sample galaxies are part of a new population of optically faint, but infrared luminous starburst galaxies. These galaxies are also characterised by an extremely high rate of evolution with redshift up to $z \sim 1.5$ and significantly contribute to the cosmic far-IR extragalactic background.

[1]ISOCAM was a mid-infrared camera, one of the four instruments on board the Infrared Space Observatory (ISO).

1. New Facts from Deep Sky Explorations at Long Wavelengths

Observations at wavelengths longer than a few μm are essential to study diffuse media in galaxies, including all kinds of atomic, ionic and molecular gases and dust grains. By definition, they are particularly suited to investigate the early phases in galaxy evolution, when a very rich ISM is present in the forming systems.

Unfortunately, the IR and sub-millimetre constitute a very difficult domain to access: astronomical observations are only possible from space, apart from a few noisy atmospheric windows at $\lambda \sim 10$ and 850 μm where they can be done from dry sites on the ground.

1.1 Discovery of the Cosmic Infrared Background

During the last few years, a variety of observational campaigns in the far-IR/sub-mm have started to provide results of strong cosmological impact, by exploiting newly implemented ground-based and space instrumentation.

One important discovery in the field during the last few years concerned an intense diffuse isotropic flux detected at far-IR/sub-mm wavelengths in the all-sky maps imaged by the Cosmic Background Explorer (Puget et al. 1996; Hauser et al. 1998). The isotropy of this background (henceforth the Cosmic IR Background, CIRB) was immediately interpreted as due to an extragalactic source population, but its intensity turned out to be far in excess of the level expected from local galaxies, as observed by IRAS and by millimetre telescopes (e.g. Franceschini et al. 1998). What is remarkable in this context is that the bolometric CIRB flux is at least a factor of two larger than the integrated stellar light from galaxies at any redshifts, as sampled by the HST in ultra-deep imaging surveys.

Then the only viable interpretation for the CIRB was to correspond to an ancient phase in the evolution of galaxies characterised by an excess emission at long wavelengths, naturally interpretable as an effect of a rich and dusty interstellar medium. The large energetic content of the CIRB compared to the optical already sets interesting constraints on galaxy evolution in very general terms, as our team will report in due course.

1.2 Deep SCUBA surveys resolve part of the CIRB at the mm

Particularly relevant have been the deep explorations performed by the

Sub-millimetre Common User Bolometer Array (SCUBA), an imaging camera operating on the JCMT mostly at 850 μm, and by the Infrared Space Observatory (ISO) over a wide wavelength interval from 5 to 200 μm.

Deep surveys by the two observatories have started to provide crucial information on faint distant infrared sources. Because of the different K-corrections, the two source selections probed rather complementary redshift intervals. SCUBA detected at 850 μm redshifted dust-emission from tens of galaxies over a wide redshift interval, mostly between $z \simeq 1$ and $z \simeq 3$, although a completely reliable identification of these faint sub-millimetric sources is still to be definitely established. The most serious limitation of this approach is due to the large error-box for faint SCUBA sources, combined with the extreme optical faintness of their majority, which imply a significant chance of misidentification.

1.3 A population of fast-evolving IR sources discovered by ISO

The IR camera (ISOCAM, P.I. C.J. Cesarsky) on board ISO, with its broad-broad-band filter LW3 sensitive between 12 and 18 μm, provided the most sensitive and spatially accurate way of sampling the far-infrared sky. While designed as an observatory-type mission, the vastly improved sensitivity offered by ISOCAM with respect to the previous IRAS surveys incited us to propose that a significant fraction of the ISO observing time be dedicated to deep surveys (ISOCAM Guaranteed Time Extragalactic Surveys, IGTES, P.I. C.J. Cesarsky). The aim was to parallel optical searches of the deep sky with complementary observations at wavelengths where dust is not only far less effective in extinguishing photons, but is even strongly emissive (in particular through a set of broad emission features peaking at $\lambda \simeq 6$ to 9 μm by as yet unidentified grain species).

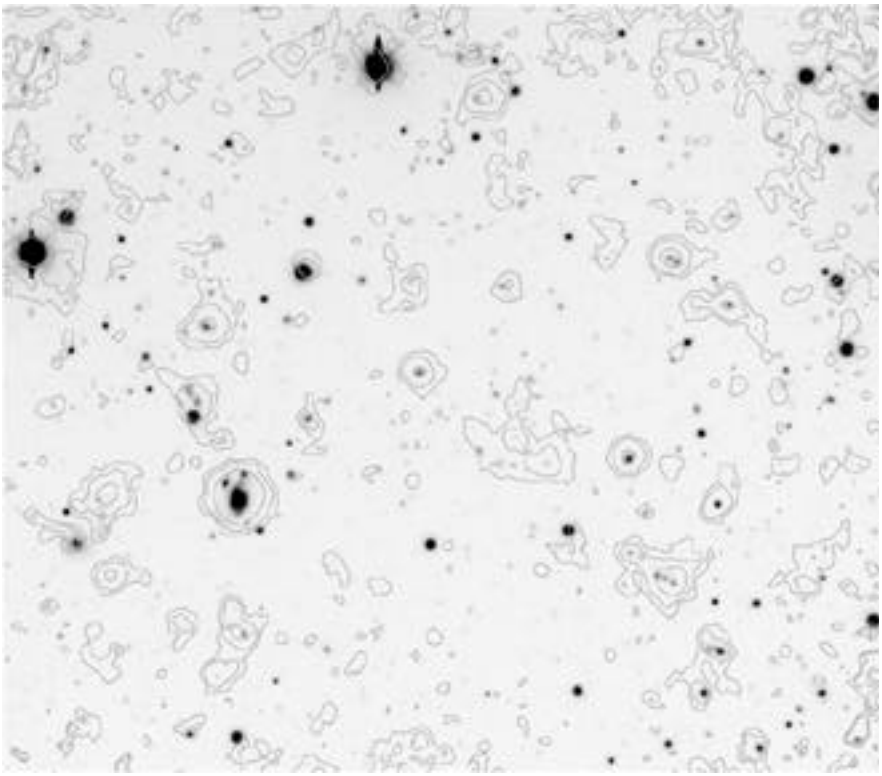

Figure 1: Contours of the ISOCAM LW3 image (15 μm, Aussel et al. 2000) overlaid on the NTT-I band image of Dennefeld et al. (2000).

Table 1. ISOCAM surveys

Name	λ (μm)	Area ($'^2$)	depth (mJy)	# objects [a]	Ref.	coord.(2000)
CAM parallel	7, 15	1.2e5	5	>10000	1	–
ELAIS	7, 15	4e4	1.3	~1000	2	–
Marano2 FIRBACK	15	2700	1.4	29	3	03 13 10 –55 03 49
Lockman Shallow	15	1944	0.72	180	4	10 52 05 +57 21 04
Comet Fields	12	360	0.5	37	5	03 05 30 –09 35 00
Lockman Deep	7, 15	500	0.3	166	6	10 52 05 +57 21 04
CFRS 14+52	7, 15	100	0.3	23, 41	7	14 17 54 +52 30 31
CFRS 03+00	7, 15	100	0.4	8		03 02 40 +00 10 21
Marano2 Deep	7, 15	900	0.19, 0.32	180	9	03 13 10 –55 03 49
A370	7, 15	31.3	0.26	18	10	02 39 50 –01 36 45
Marano Ultra-deep	7, 15	90	0.14	142	11	03 14 44 –55 19 35
Marano2 Ultra-deep	7, 15	90	0.1	115, 137	12	03 13 10 –55 03 49
A2218	7, 15	16	0.12	23	10	16 35 54 +66 13 00
ISOHDF South	7, 15	25	0.1	63	13	22 32 55 –60 33 18
ISOHDF North	7, 15	24	0.05, 0.1	7, 44	14	12 36 49 +62 12 58
Deep SSA13	7	9			15	13 12 26 +42 44 24
Lockman PG	7	9	0.034	15	16	10 33 55 +57 46 18
A2390	7, 15	5.3	0.030	32, 31	17	21 53 34 +17 40 11

[a] If only one number appears, it refers to the longer-λ survey.

References: (1) Siebenmorgen et al. (1996); (2) Oliver et al. (1999); (3), (4), (6), (9), (11), (12): IGTES, see Elbaz et al. (1999); (5) Clements et al. (1999); (7), (8): Flores et al. (1999); (10): Altieri et al. (1999); (13) Elbaz, D., et al, (1999); Oliver et al. submitted (14) Aussel, H., et al. (1999); (16) Taniguchi et al. (1997).

Careful corrections of some transient effects in the detector responsivity (due to the very low temperature and slow electron mobility) and of the non-gaussian noise induced by cosmic-ray impacts are now possible using various independent methods (PRETI developed at the Service d'Astrophysique de Saclay, Stark et al. 1998; a method developed in Bologna by Lari et al. 2000; and one by Desert et al. 1998), all providing consistent results. All this required quite an extensive amount of work (including Monte Carlo simulations of the complex behaviour of the detectors) and fairly long time, but eventually we are in a position to claim that we have now an accurate sampling in the LW3 filter of several independent sky areas down to very faint flux densities and producing highly reliable and complete source catalogues including more than one thousand sources (Elbaz et al. 1999). We report in Table 1 a summary of the surveys performed with ISOCAM during the 2.5 years of the mission lifetime.

An example of the imaging quality achieved is reported in Figure 1, which is the LW3 map of an area centred on the Hubble Deep Field South (Aussel et al. 2000a).

The Euclidean-normalised differential counts provide simple but powerful and robust statistics, useful to evidenciate evolutionary properties in the selected sources. A collection of the LW3 differential counts is reported in Figure 2 based on eight samples of independent sky areas. The first remark is that the counts from all of them are

nicely consistent and support within the statistical uncertainties the accuracy of the adopted methods for source selection. The fact that the observed counts are a factor ten higher around a flux density of 0.3–0.4 mJy provides the first uncontroversial evidence for a drastic increase of the far-infrared emissivity of galaxies going back in cosmic time.

This result is quite consistent with the independent evidence, provided by the CIRB intensity, in favour of very rapid evolution of IR flux from cosmic sources. Indeed, by assuming for the faint ISOCAM sources in Figure 2 the far-IR spectrum of a typical starburst, then these sources would be expected to contribute a substantial part of the CIRB at 140 microns.

Aussel et al. (1998) and Flores et al. (1998) have produced early attempts to identify the ISOCAM sources and to derive their redshifts at the fluxes where the peak excess in the LW3 counts of Figure 2 is observed. Mostly due to the combined effect of K-correction and evolution, these sources are found to range from $z \sim 0.4$ to $z \sim 1.2$, with a median around $z = 0.7$–0.8 (see below).

However, the origin of this energy, either due to stellar nucleosynthesis in star-forming galaxies or to gravitational accretion onto giant black holes as in quasars, is largely unknown. We clearly need a deep spectroscopic survey of these sources to progress in their understanding.

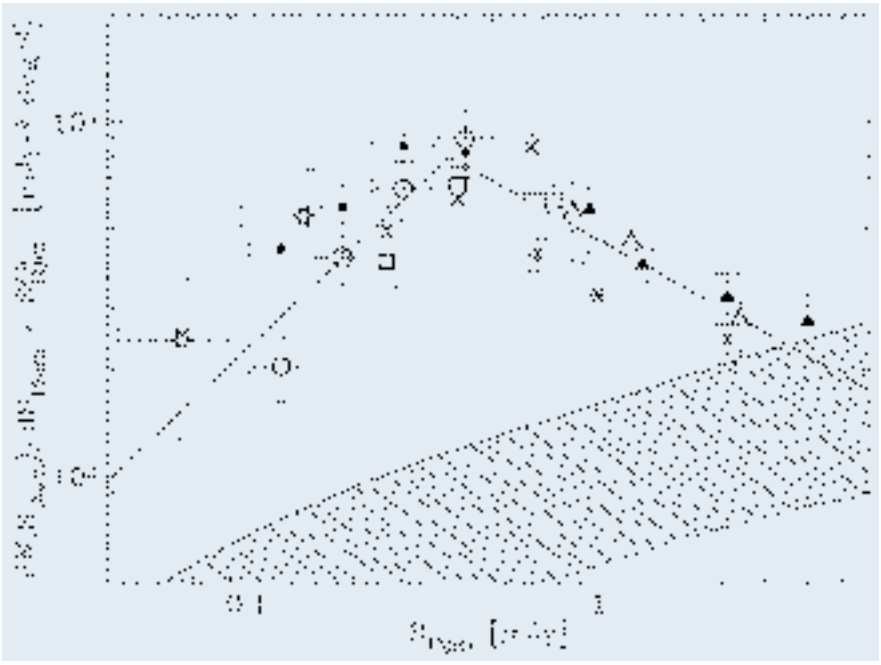

Figure 2: Differential number counts from eight different ISOCAM surveys (from Elbaz et al. 1999).

2. The ISOCAM Survey in the HDFS

The Hubble Deep Field South was observed by ISOCAM at two wavelengths, LW2 (6.75 μm) and LW3 (15 μm), as part of the European Large Area ISO Survey (P.I. M. Rowan-Robinson; see Oliver et al. 2000). ISOCAM detected 63 sources (from the data reduction of Aussel et al. 2000), all brighter than $S_{15\mu m} = 100$ μJy in the LW3 band. Out of this source list we selected the sample for ISAAC follow-up. The selected sources satisfied the following criteria:
(a) they had a reliable LW3 detection, (b) Hα in the wavelength range of ISAAC and, (c) a secure counterpart in the I-band image (Dennefeld et al. 2000) and/or in the K-band image (ESO-EIS Deep, DaCosta et al. 1998). The reference sample contains about 25 galaxies with 15 μm flux densities in the range 100–800 μJy and is therefore a fair representation of the strongly evolving ISOCAM population near the peak of the differential source counts (Elbaz et al. 1999). From these 25 sources we selected randomly 12 sources for our first ISAAC follow-up spectroscopy (hereafter ISOHDFS galaxies).

For the observations and the selection of the exact near-infrared band (Z, SZ, J or H) we used spectroscopic redshifts from optical spectra, where available for $z < 0.7$ (Dennefeld et al. 2000)

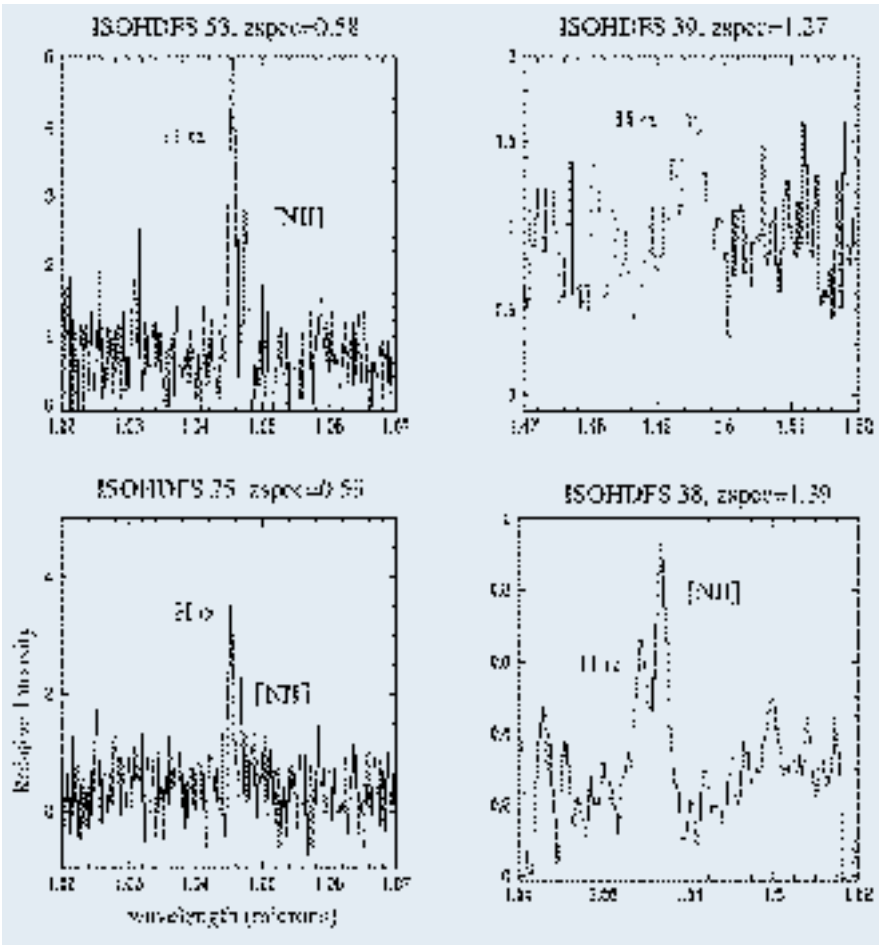

Figure 3: ISAAC-VLT spectra of ISOCAM galaxies, showing two low-z and two high-z sources. The resolution of 600 corresponds to a resolution of about 12Å at the source distance. The H_α and [NII] lines are resolved in three of the spectra. Clockwise from top left: source ISOHDFS 53, at $z_{spec} = 0.58$, source ISOHDFS 39 at $z_{spec} = 1.27$, source ISOHDFS 25 at $z_{spec} = 0.59$, and source ISOHDFS 38 at $z_{spec} = 1.39$ (the H_α/[NII] < 1 implies that this source is an AGN) (spectra from Rigopoulou et al., 2000). ▶

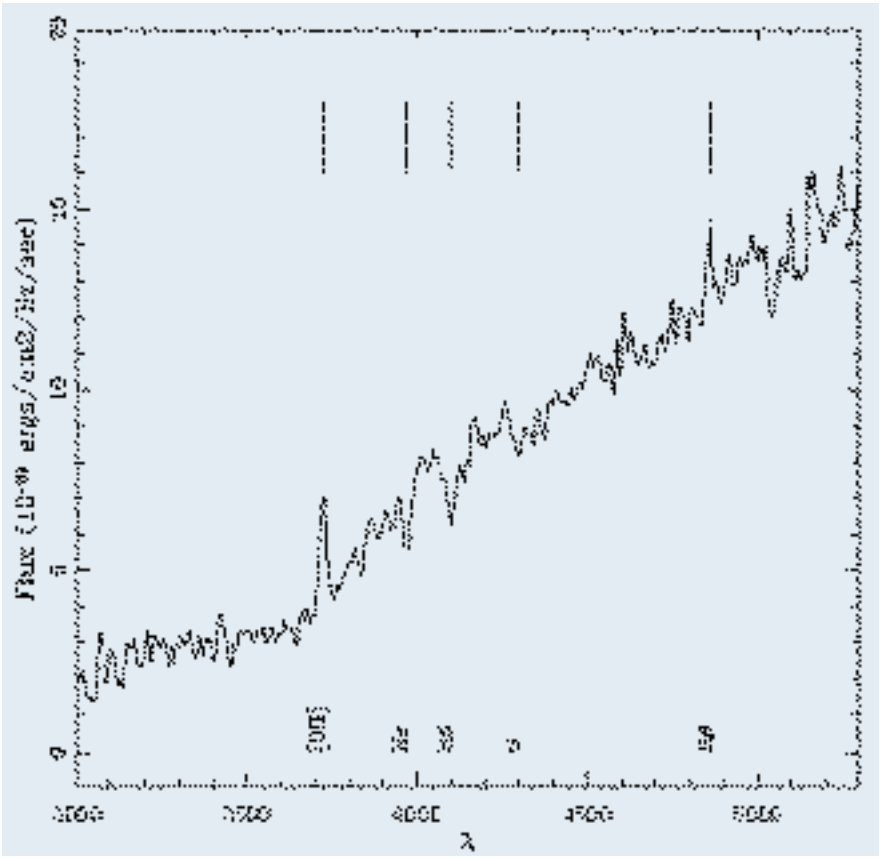

Figure 4: Restframe B-band "averaged" spectrum of ISOCAM galaxies from the CFRS field (from Flores et al. 1999). H_δ and H_ε Balmer absorption features are prominent, alongside a moderately strong [OII] emission.

or photometric redshift estimates. Photometric redshifts have been estimated by using the model PEGASE (Fioc and Rocca-Volmerange 1997). Our photometric redshift determination turned out to be accurate to $\Delta z = \pm 0.1$ and provided a very useful tool for the ISAAC follow-up spectroscopy.

3. The ISAAC Observations

We carried out observations (P.I. A. Franceschini) during 20–24 September 1999 (we observed during the first half of the night). The seeing varied between 0.4–1.00 arcsec and the conditions were generally very good. The good seeing helped us to acquire the very faint objects relatively quickly, our elementary integrations consisted of 1–2 minutes exposure in the H-band. For the observations we used the low-resolution grating $R_s \sim 600$ and a 1-arcsec × 2-arc min long slit. We positioned the slit in such a way as to include on average two galaxies at any given orientation. The choice of filter was dictated by our aim to detect the Hα emission line. Based on the redshift information we had at hand (photometric or spectroscopic) we used the Z (0.83–0.97 μm), SZ (0.98–1.14 μm), J (1.1–1.39 μm) or H (1.42–1.83 μm) filters accordingly.

The H magnitude of our targets (taken from the ESO-EIS Deep) reached down to 22 mag. The very faint objects were acquired by offsetting from a bright star in the field. The individual exposures ranged from 2 to 4 minutes. Most of the spectra were acquired within 1 hour, except for the very faint ones ($H \geq 20.5$ mag) for which we integrated for nearly 2 hours. For each filter, observations of spectroscopic standard stars were made in order to flux calibrate the spectra. The data were reduced using several ECLIPSE applications (Devillard 1998) and standard routines from the IRAF package. We extracted spectra using IRAF-APEXTRACT.

In total we observed 12 galaxies and H_α was successfully detected in all but one of them. [NII] emission is also seen in some spectra. Figure 3 shows some representative spectra.

4. Nature of the Faint ISOCAM Galaxies

Prior to our VLT-ISAAC observations no near-infrared (rest-frame R-band) spectroscopy had been carried out for the ISOCAM population, mostly due to the faintness of the galaxies. Optical spectroscopy (rest-frame B-band) has been done for Hubble Deep Field North (Barger et al. 1999) and the Canada France Redshift Survey (CFRS) field (Flores et al. 1999). The ISOCAM HDF-N galaxies have been cross-correlated with the optical catalog of Barger et al. (1999) resulting in 38 galaxies with confirmed spectroscopic redshifts (Aussel et al. 1999). Flores et al. have identified 22 galaxies with confirmed spectroscopic information. In both of these samples the median redshift is about 0.7–0.8. Our VLT ISOHDFS sample contains 7 galaxies $0.4 < z < 0.7$ and 5 galaxies with $0.7 < z < 1.4$. Thus our sample has a z-distribution very similar to the HDF-N (Aussel et al.) and CFRS (Flores et al.) samples.

Rest-frame B-band spectra host a number of emission and absorption lines related to the properties of the starburst in a galaxy. Based on these features, galaxies can be classified according to their starburst history. Strong H_δ, H_ε Balmer absorption and no emission lines are characteristic of passively evolving k+A galaxies. The presence of significant higher level Balmer absorption lines implies the presence of a dominating A-star population. Such an A-star population may have been created in a burst 0.1–1 Gyr ago (post-starbursts). The simultaneous presence of Balmer absorption and moderate [OII] emission, known as e(a) galaxies, may be characteristic of somewhat younger, but still post-starburst systems or, alternatively, an active but highly dust absorbed tar-bursts. As we will show, the ISOCAM galaxies are in fact powerful starbursts hidden by large amounts of extinction.

Figure 4 shows the average B-band spectrum of the CFRS galaxies (from Flores et al. 1999). The spectrum shows moderate [OII] emission and quite prominent deep Balmer absorption features H_δ, H_ε reminiscent of A stars. Based on this spectrum, Flores et al. suggested that these galaxies look like post-starburst systems. In Figure 5 we plot the B-band and R-band spectrum of the well-known starburst galaxy M82 (spectra from Kennicutt 1992). We note a very similar behaviour: the B-band spectrum of M82 displays characteristics of an e(a) system. At the same time the R-band spectrum displays strong H_α emission with large equivalent widths implying an active on-going star formation. Differential extinction lies at the heart of this apparent disagreement (Poggianti et al 2000): large amounts of dust exist within the HII regions where the H_α and [OII] line emission originates. [OII] emission is affected more than H_α simply because of its shorter wavelength. The continuum is due to A-stars. This A-star signature comes from earlier (0.1–1.0 Gyr) star-formation activity that is not energetically dominant; in fact, it plays a small role once the dusty starburst is dereddened. Such a scenario implies that these galaxies undergo multiple burst events: the less extincted population is due to an older burst while in the heavily dust enshrouded HII regions there is ongoing star formation. Therefore, ISOCAM galaxies are actively star-forming,

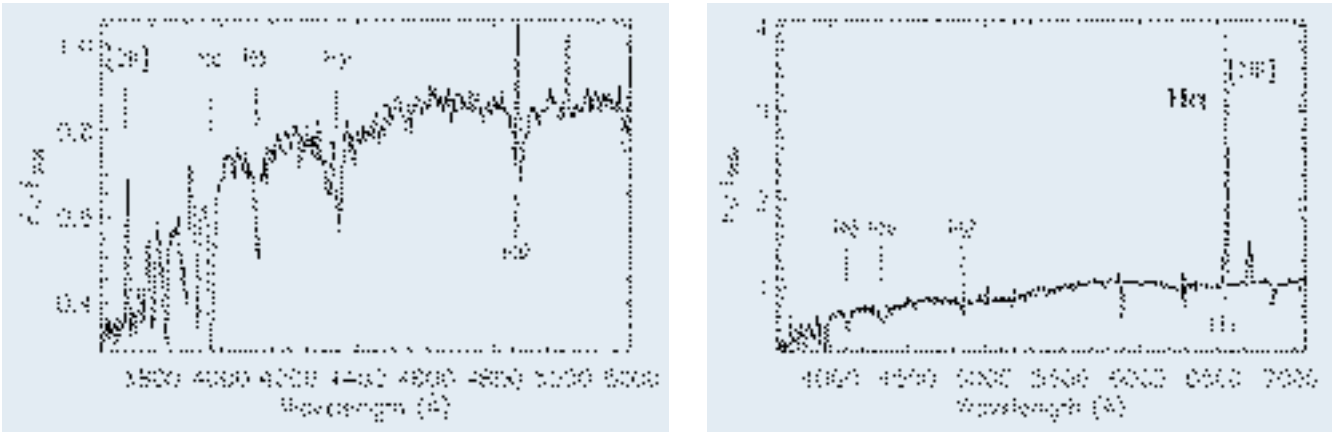

Figure 5: Left panel: B-band spectrum of the well-known starburst galaxy M82. Note the prominent Balmer H_δ and H_ε absorption lines as well as the moderate [OII] emission. Right panel: R-band spectrum of M82. The spectrum is dominated by the very strong H_α emission (spectra from Kennicutt 1992).

dust-enshrouded galaxies, akin to local LIRGs (e.g. NGC 3256, Rigopoulou et al. 1996).

5. Evaluating the Star Formation Activity

Being the strongest of all Balmer lines, the H_α emission line has been traditionally used to derive quantitative star-formation rates in galaxies. However, for $z \geq 0.2$–0.3, H_α redshifts into the near-infrared where spectroscopy with 4-m-class telescopes is inherently much harder and thus less sensitive than in the optical. This is why measurements of the star-formation rates in high redshift galaxies have relied on measurements of the [OII] λ3727 doublet. The advent of 8-m-class telescopes such as the VLT allows us for the first time to use H_α as a measure of the star-formation activity in distant galaxies.

In ionisation bounded HII regions, the H_α luminosity scales directly with the ionising luminosity of the embedded stars and is thus proportional to the star-formation rate (SFR). The conversion factor between ionising luminosity and SFR is computed with the aid of an evolutionary synthesis model. The prime contributors to the integrated ionising flux are massive stars ($M > 20\ M_\odot$) with relatively short lifetimes (≤ 10 million years). Using any stellar synthesis model (we have used the code of Sternberg 1998) for solar abundances, a Salpeter IMF (1–100 $M_\odot$) and for a short-duration burst (a few 10^7 yrs) we obtain:

$$SFR(M_\odot/yr) = 5 \times 10^{-42} L(H_\alpha)(ergs^{-1}). \quad (1)$$

Using this formula we estimate that the SFR rates in our ISOHDFS galaxies range between 2–50 $M_\odot$/yr, corresponding to total luminosities of ~ 1–10 × 10^{42} erg s^{-1} (assuming $H_0 = 50$ km/s/Mpc, $\Omega = 0.3$).

The SFR estimates based on eq. (1) represent only a *lower limit* of the real SFR in these galaxies. To get an estimate of the extinction, we use V–K colour indices (magnitudes taken from the ESO-EIS survey) and using STARBURST99, the evolutionary synthesis code of Leitherer et al. (1999), for various star-formation histories we calculated the range of intrinsic (extinction-free) colours. By comparing the observed V–K colours to the model-predicted ones we derive a median extinction A_V of 1.8 assuming a screen model for the extinction. This A_V value corresponds to a median correction factor for the SFR(H_α) of ~ 4.

But the far-infrared luminosities can also be used to infer SFR, especially since the ISO-HDFS galaxies are dust enshrouded. For the same IMF as above, the SFR scales with the FIR luminosity as:

$$SFR(M_\odot/yr) = 2.6 \times 10^{-44} L_{FIR}(ergs^{-1}) \quad (2)$$

The L(FIR) in equation (2) is calculated based on the method of Franceschini et al. (2000) which uses the 15 μm flux and assumes an L_{FIR}/L_{MIR} ratio of ~ 10. We find that the SFR(FIR) estimates are on average a factor of 5 to 50 higher than the SFR estimates inferred from H_α uncorrected for extinction. The ratio SFR(FIR)/SFR(H_α) drops to 3 if we use extinction-corrected H_α values, confirming that the extinction in these galaxies is much higher than inferred from UV or optical observations alone. Thus, ISOCAM galaxies are in fact actively star-forming dust-enshrouded galaxies. We finally note that the factor 3 inconsistency noted above for the FIR-based SFR is consistent with the value obtained by Poggianti et al. (2000) for a sample of luminous IRAS starbursts.

6. Conclusions and Future Plans

We have obtained the first near-infrared spectra (rest-frame R-band) of a sample of 12 ISO selected far-IR galaxies from the Hubble Deep Field South. The detection of strong H_α emission lines with large EW in all but one is consistent with these ISOCAM sources being powerful dust enshrouded starburst galaxies.

In only one object (see Fig. 3) we find evidence for the presence of an AGN, as inferred from the inverted NII/H_α line ratio and the peculiar and high 6.7 μm to 15 μm flux ratio, indicative of very hot AGN-like dust. In general, we do not find evidence for broad H_α components as would be expected from classical AGNs, but this will require further NIR spectra at high resolution for confirmation. Our result echoes recent reports about ultra-deep CHANDRA hard X-ray surveys of high-*z* SCUBA sources, in which no high-X-ray-energy emission was detected as would be expected if even a fraction of the FIR flux would be due to an AGN (Hornschemeier et al. 2000). Generalising these results, we may tentatively conclude that the large energy content of the CIRB originates from stellar activity.

Based on the H_α emission line intensity we estimate star-formation rates in the range 2–50 $M_\odot$/yr, which are a factor of 5–50 times lower than the SFR we derive based on FIR luminosities. If we correct the H_α for extinction, we deduce SFR(FIR)/SFR(H_α) ~ 3, confirming that the extinction in the ISOCAM galaxies is much higher than can be predicted using UV or optical data alone. This result demonstrates that deriving star-formation rates from UV/optical data alone is incorrect for this class of sources. A fraction of star formation, hard to quantify at the moment but probably quite significant, is entirely missed by optical surveys.

We plan to continue our project by increasing our statistics on ISOCAM galaxies. In our upcoming August 2000 run we will supplement our sample with low-resolution spectroscopy of new ISOCAM targets. Meanwhile, we will also attempt to obtain higher-resolution spectra to probe the gas kinematics and ionisation stage in these galaxies.

The unique combination offered by ISO and ISAAC instruments promises a decisive progress in our understanding of the origin of the vast amount of energy released by starburst galaxies during their main activity phases.

References

Altieri, B., et al., 1999, *A&A* **343**, L65.
Aussel, H., Elbaz, D., Cesarsky, C.J., Starck, J.L., 1999, In The Universe as seen by ISO, eds. P. Cox, M.F. Kessler, ESA SP **47**, 1023.
Aussel, H., Cesarsky, C.J., Elbaz, D. and Starck, J.L.,1999, *A&A* **342**, 313.
Aussel, H. et al., in preparation.
Da Costa et al., 1998, *http://www.eso.org/science/eis/eis-rel/deep/HDF-Srel.html*
Clements, D., et al., 1999, *A&A* **346**, 383.
Dennefeld et al. 2000, in prep.
Devillard N., 1998, *The Messenger* No. **87**, March 1997.
Desert, F.X., et al., 1999, *A&A* **342**, 363.
Elbaz, D., Cesarsky, C.J., Fadda, D., Aussel, H., et al. 1999 *A&A* **351**, L37.
Fioc, M., Rocca-Volmerange, B., 1997, *A&A* **326**, 950.
Flores, H., Hammer, F., Thuan, T.X., Cesarsky, C., 1999 *Ap.J.*, **517**, 148.
Franceschini et al. (2000) in prep.
Kennicutt, R.C., (1992) *Ap.J.*, **388**, 310.
Hornschemeier, A.E., et al., 2000, astroph/0004260.
Lari, C., et al., 2000, in prep.
Leitherer, C., et al., 1999 *ApJS* **123**, 3.
Oliver, S., et al., 2000., in prep.
Oliver, S., et al., 2000, MNRAS, in press, astroph.
Poggianti B., Bressan A., Franceschini A., 2000, *ApJL* submitted.
Rigopoulou, D., et al, 1996, *A&A*, **305**, 747.
Rigopoulou, D., Franceschini, A., Aussel, H., et al. 2000, *ApJL,* in press.
Siebenmorgen, R., et al., 1996, *A&A* **315**, L169.
Starck, J.L., et al., *A&A* **134**, 135.
Sternberg, A., 1998, *ApJ* **506**, 721.
Taniguchi,Y., Cowie, L.L., Sato, Y., Sanders, D.B., et al., 1997, *A&A* **318**, 1.

The Deep Eclipse of NN Ser

R. HÄFNER, Universitäts-Sternwarte München

The elusive nature of NN Ser was discovered in July 1988 (Häfner, 1989a, 1989b) in the course of a search for eclipses in faint cataclysmic variables using the CCD camera on the Danish 1.5-m telescope at La Silla. This target (V ~ 17), then named PG 1550+131 and thought to be such a variable, turned out to exhibit a sine-shaped light curve and a very deep eclipse of short duration repeating once every 3 hours and 7 minutes. Due to the low time resolution of the photometry (3.5 min), the duration of the eclipse (separated by half a period from maximum light) as well as its depth could only be roughly estimated to be about 12 min and at least 4.8 mag respectively. During mid-eclipse no signal from the object was recordable. Two spectra (resolution about 12 Å) obtained near maximum light (A) and near the onset of the eclipse (B) using EFOSC at the 3.6-m telescope revealed mainly narrow emission lines of the Balmer series superimposed on broad absorptions (A) and shallow Balmer absorptions without emission (B). It was immediately clear that such an object could not be a cataclysmic system. The data were rather interpreted in terms of a pre-cataclysmic binary, an evolutionary precursor of a cataclysmic system, consisting of a white dwarf/late main-sequence detached pair. Thus all observed properties of the system find a consistent explanation: the sine-shaped light curve (full amplitude ~ 0.6 mag) is caused by a strong heating effect, the emission lines originate in the heated hemisphere of the cool star and cannot be seen near primary eclipse, the absorption lines originate in the hot star, the steep (ingress/egress ~ 2 min) and deep eclipse of short duration are due to the obscuration of a very hot small object by a much cooler and larger star, a secondary eclipse is not detectable since the cool star does not contribute much to the flux. Based on these observations and assuming M_{hot} = 0.58 $M_\odot$ (mean value for DAwhite dwarfs), T_{hot} = 18,000 K, inclination close to 90º and a circular orbit, a first crude estimate of the system parameters yielded the following results: separation ~ 0.92–1.03 $R_\odot$, R_{hot} ~ 0.01–0.14 $R_\odot$, R_{cool} ~ 0.06–0.33 $R_\odot$, M_{cool} ~ 0.03–0.28 $M_\odot$, T_{cool} (unheated hemisphere) ~ 2600–3300 K, T_{cool} (heated hemisphere) ~ 4300–6600 K, spectral type of cool star ~ M3–M6. The evolution of the system into the semi-detached (cataclysmic) state is only possible via radiation of gravitational waves and was estimated to take some 10^9 years.

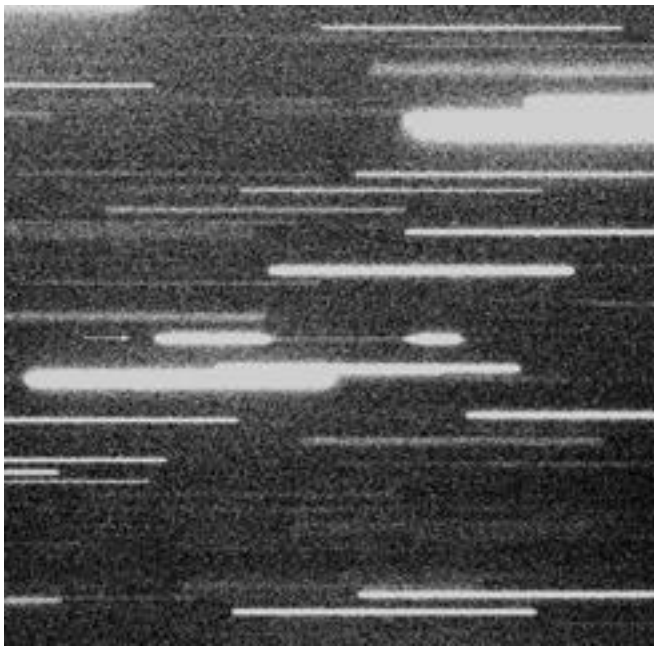

Figure 1: The drift exposure of the sky field around NN Ser (arrow).

Based on optical and IUE spectroscopy as well as further photometry (Wood and Marsh, 1991; Catalan et al., 1994), the pre-cataclysmic nature of NN Ser was confirmed and the range of system parameters could be narrowed down. The IUE data as well as fits of some Balmer absorptions via model atmospheres hint at a white dwarf temperature in the range 47,000–63,000 K, much more than previously assumed. But all studies so far performed were hampered by the fact that the true depth of the eclipse and the duration of the totality (if any), i.e. the inner contact phases of the white dwarf, were not known. This crucial information, important for the determination of the radii of the components, could not be obtained using telescopes of the 4-m class, as several attempts by the author revealed. Even applying sophisticated observing methods and/or using a special photometer, several observing runs (ESO 3.6-m telescope, NTT and Calar Alto 3.5-m telescope) were not successful in this respect.

The powerful combination of the first VLT 8.2-m Unit Telescope (ANTU) and the multi-mode FORS1 instrument (Appenzeller et al., 1998) offered now the opportunity for a new experiment. Since the HIT mode, allowing photometry and spectroscopy with high time resolution, was not yet available at the scheduled time of observation (June 1999) another technique had to be applied: the trailing method, where the tel-